Spatiotemporal precipitation trends and associated large-scale teleconnections in northern Pakistan

Ansa Rebi[1,2,†], Azfar Hussain[3,†], Ishtiaq Hussain[4], Jianhua Cao[3], Waheed Ullah[5], Haider Abbas[6], Safi Ullah[7], Jinxing Zhou[1,2,*]

[1] Jianshui Research Station, School of Soil and Water Conservation, Beijing Forestry University, Beijing 100083, China

[2] Key Laboratory of State Forestry and Grassland Administration on Soil and Water Conservation, Beijing Forestry University, Beijing 100083, China

[3] International Research Center on Karst under the auspices of UNESCO; Institute of Karst Geology, Chinese Academy of Geological Sciences, Guilin 541004, China

[4] Department of Applied Mathematics, Chung Yuan Christian University Chung-Li 541004, Taiwan

[5] Defense and Security, Rabdan Academy, Abu Dhabi 114646, United Arab Emirates

[6] Synthesis Research Centre of Chinese Ecosystem Research Network, Key Laboratory of Ecosystem Network Observation and Modelling, Institute of Geographic Sciences and Natural Resources Research, Chinese Academy of Sciences, Beijing 100101, China

[7] Department of Atmospheric and Oceanic Sciences and & Institute of Atmospheric Sciences, Fudan University, Shanghai 200433, China

[†]These authors contributed equally to this work.

[*] Corresponding author: Jinxing Zhou, School of Soil and Water Conservation, Beijing Forestry University, Beijing 100083, China.
Email: zjx001@bjfu.edu.cn; ORCID: https://orcid.org/0000-0003-2182-9849

Abstract. The effects of climate change are unparalleled in magnitude, ranging from changing weather patterns that endanger food production to increasing sea levels that increase the likelihood of catastrophic flooding. Therefore, the extent of such variations on regional and local is imperative. We used monthly precipitation data from 25 meteorological stations in northern Pakistan (NP) to document the observed changes in seasonal and annual precipitation. The station density in the NP is small and unevenly distributed; therefore, ERA-5 reanalysis data are used to supplement the observed dataset to assess the spatial trends in NP. The non-parametric Mann-Kendall (MK), Sen's Slope estimator (SSE), and Sequential Mann-Kendall (SQMK) tests were performed to assess the trends. In addition, the wavelet analysis technique was used to determine the association of precipitation with various oceanic indices from 1960 to 2016. Results indicate that maximum precipitation was shown in the annual and summer seasons. In NP, annual, winter, spring, and summer precipitation declined, while an increase in autumn was observed at a rate of 0.43 mm/decade between 1989 and 2016. The spatial trends for observed and ERA-5 reanalysis datasets are almost similar in winter, spring, and autumn; however, some disagreement is observed in both datasets in the summer and annual precipitation trends in NP during 1960−2016. Between 1989 and 2016, summer and annual precipitation increased significantly in Region III. However, seasonal and annual precipitation decreased in NP between 1960 and 2016. Moreover no prominent trends in annual precipitation until the mid-1980s, but an apparent increase from 1985 onwards. Annual precipitation has increased in all elevations except at the 500 m – 1000 m zone. ENSO (El Niño-Southern Oscillation) shared notable interannual coherences among all indices above 16–64 months. Inter-decadal coherence with ENSO, AO (Arctic Oscillation), and PDO (Pacific Decadal Oscillation) in NP for 128 months and above. Generally, AO, AMO (Atlantic Multidecadal Oscillation), and NAO (North Atlantic Oscillation) exhibit less coherence with precipitation in NP. The regression of seasonal and annual precipitation reveals that winter and spring precipitation have higher linear regression with AO and ENSO, respectively, while both AO and ENSO are also dominated at the annual scale. Similarly, the IOD, and PDO indices have a higher influence in summer precipitation. The findings could help water resource managers and climate researchers develop a contingency plan for better water resource management policies in the face of changing climate change in Pakistan, particularly in the NP.

Keywords: Precipitation, Cluster analysis, Wavelet coherence, Oceanic indices, northern Pakistan

1. Introduction

Precipitation is an essential variable that significantly impacts the global climate system and energy cycle [1], i.e., hydrological, ecological, and biochemical processes [2]. Global warming directly influences the spatial and temporal variability of precipitation [3]. Climate variability in different climate zones varies due to substantial variances in the climatic backdrop, various driving forces, and regional peculiarities [4,5]. So, having good knowledge of precipitation amounts that reach the land surface is crucial to assess fresh water and managing hydrology, agriculture, and land use, including flood and drought risk [6-8]. Therefore, quantifying the trends and variabilities in precipitation on a regional scale is of paramount concern [4,9].

Due to complex topography, dynamic climatology, and inadequate coping capacity, Pakistan is one of the most vulnerable countries to climate change [10,11]. It is among the top ten countries, most affected by extreme climate events [12,13]. Climate change has significantly affected the spatiotemporal variability of precipitation in Pakistan [14]. This variability affects the availability of water resources, resulting in hydrometeorological disasters in the country [15,16]. Recent floods (in 2010) and prolonged drought (from 1997 to 2002) are examples of climate-related extremes that affected millions of people nationwide. The northern highlands of Pakistan are prone to floods [17], whereas the southern areas are drought-prone [18].

Numerous previous studies have highlighted the dynamic variability of precipitation in different parts of Pakistan. For example, Hartman 2012 reported a decreasing trend of precipitation in the western part of the Indus Basin and an increasing trend in the northern and eastern parts [19]. Similarly, increasing seasonal and annual precipitation trends were observed in the Upper Indus Basin (UIB) [20]. An increase in annual precipitation in the Himalayan region was reported by Adnan et al. [21] and Gadiwala et al. [22]. An annual and significant seasonal increase was observed in the Swat Basin [23].

Considering the association of global teleconnections with precipitation in northern Pakistan (NP), Iqbal and Hussain [24] explored the influence of ocean-atmospheric circulations on precipitation during 1976−2013 and observed that the NAO, ENSO, and PDO influenced precipitation in the Azad Jammu and Kashmir, while IOD, ENSO, NAO, and ENSO influenced precipitation in Khyber Pakhtunkhwa. Afzal et al. [25] investigated the influence of NAO and ENSO on winter precipitation in NP and found that NAO is less influential than ENSO, and observed that precipitation remained normal in this region with the positive phase of the NAO and the negative phase of the ENSO. Hussain et al. [20] examined precipitation variation and the influence of climate indices on precipitation in the UIB and observed that the PDO showed less significant results. In contrast, ENSO showed significant results as compared to NAO and IOD. The combined interaction of the Pacific Ocean and the atmosphere affects the strength and location of the westerly jet, which gives shape to the western disturbance via teleconnection that, intrudes Pakistan from the west [26]. According to Lau and Kim [17], the Russian heatwave was due to blocking extratropical atmospheric events linked with atmospheric Rossby wave trains over central Asia and the Tibetan Plateau.

After a detailed literature review on variability, trends, and teleconnections, the region needs a more intensive and organized analysis of precipitation variations over its various homogenous climatic regions and their associations with large-scale oceanic indices. Whether NP's seasonal and annual precipitation trends are changing due to climate change, need detailed and systematic evaluation. Furthermore, there have been few investigations on the effects of precipitation variation in this region [19,27]. Despite the significant impact of climate change on precipitation patterns and associated consequences for water resources management and agriculture in northern Pakistan, there is a lack of research on the spatiotemporal trends of precipitation over homogenous climatic regions and their relationship with large-scale mechanisms. Previous studies have focused on the overall precipitation trends without considering the homogenous regions, which may provide valuable insights for effective water resource planning and management. Additionally, few studies have explored the potential links between precipitation trends

in northern Pakistan and large-scale influencing mechanisms, such as the El Niño-Southern Oscillation (ENSO) and the Indian Ocean Dipole (IOD), which are known for their significant influence on the regional climate. Therefore, this study aims: (1) to identify the homogenous precipitation regions using cluster analysis, (2) to assess the spatial and temporal trend of seasonal and annual precipitation from 1960 to 2016, and (3) to investigate the association between large-scale climate indices, i.e., AMO, AO, NAO, ENSO, PDO, and PNA. The findings of this study could help water resource managers and climate scientists to develop a contingency plan for better water resource management in the face of changing climate change.

Figure 1. Spatial distribution of meteorological stations in different sub-basins in northern Pakistan. The red outline indicates the boundary of the Upper Indus basin with the administration of northern Pakistan.

2. Study Area

Pakistan has subtropical to a tropical climate, with a latitudinal range of 23 to 37 degrees north and a longitudinal span of 61 to 78 degrees east [28]. The highest elevation is about 8611m, the world's second-highest mountain (K-2) [20]. The geography of Pakistan is diverse, having high peaks in the upper reaches, flat agricultural terrain in the middle, and a coastal belt in the lower reaches [29]. Pakistan's total mean annual precipitation is 481 mm [30]. NP's primary precipitation sources are monsoon winds and western disturbances [31]. Western disturbance originating from the Mediterranean region brings winter precipitation to NP [32,33], whereas monsoon winds arise from the Indian Ocean and the Bay of Bengal due to the difference in temperature between land and ocean. Precipitation is abundant in the NP, including upper Khyber Pakhtunkhwa (KPK) and Kashmir [34]. It plays a crucial role in agricultural and economic activities in Pakistan [35]. Agriculture is primarily climate-dependent, with each region having its crops and fruits suited to its climate [36,37]. The country's most important crops and fruits are cultivated in the summer season in various places depending on the environment [38].

Table 1. A detailed description of the selected meteorological stations in northern Pakistan.

No	Code	Stations	Region	Duration	Elevation (m)	Latitude	Longitude	Coefficient of variance
1	Nlt	Naltar	I	1995–2012	2858	36.17	74.18	0.19
2	Zrt	Ziarat		1995–2012	3669	36.49	74.26	0.51

3	Khu	Khunjerab		1995–2012	4730	36.84	75.42	0.31
4	Ast	Astor		1960–2016	2168	35.35	74.86	0.25
5	Bun	Bunji		1960–2016	1372	35.67	74.63	0.44
6	Chl	Chilas		1960–2016	1250	35.42	74.1	0.48
7	Glt	Gilgit		1960–2016	1460	35.92	74.33	0.35
8	Gup	Gupis		1960–2016	2156	36.17	73.4	0.73
9	Skd	Skardu		1960–2016	2317	35.18	75.68	0.51
10	Cht	Chitral		1964–2016	1498	35.83	71.78	0.28
11	Drh	Drosh		1960–2016	1465	35.55	71.85	0.24
12	Dir	Dir		1967–2016	1375	35.2	71.85	0.19
13	Sad	Saidu Sharif		1974–2016	961	34.73	72.35	0.22
14	Gdp	Garhi Dupatta		1960–2016	813	34.13	73.47	0.19
15	Ktl	Kotli		1960–2016	614	33.31	73.54	0.21
16	Mzf	Muzaffarabad	II	1960–2016	838	34.37	73.48	0.17
17	Blk	Balakot		1960–2016	995	34.55	73.21	0.22
18	Mur	Murree		1960–2016	2134	33.90	73.40	0.17
19	Kak	Kakul		1960–2016	1775	34.18	73.15	0.14
20	Cht	Cherat		1960–2016	1372	33.92	71.9	0.34
21	Isb	Islamabad		1960–2016	508	33.80	73.08	0.25
22	Pch	Parachinar		1960–2016	1775	33.90	70.10	0.42
23	Psh	Peshawar	III	1960–2016	328	34.02	71.58	0.34
24	Rsp	Risalpur		1960–2016	304	34.07	71.98	0.29
25	Kht	Kohat		1960–2016	564	33.45	71.53	0.31

3. Materials and Methods

3.1. Dataset and preprocessing

The Pakistan Metrological Department (PMD) provided monthly precipitation data from 1960 to 2016 (Figure 1 and Table 1). These stations are not evenly distributed all over NP, and the number of stations covering this region is very small. Therefore, we also used ERA-5 reanalysis data along with the station data to assess the precipitation trends in the whole region for the study period. ERA-5 precipitation datasets can be used as an alternative to observed data due to its better performance [39]. The PMD collects, compiles, and screens all metrological variables to ensure quality. A standardized normal homogeneity test (SNHT) approach was used for homogeneity testing [40]. This approach was used to decrease the influence of non-climatic factors on climate series [41,42]. The relative and standalone tests were also used for this purpose. Autocorrelation analysis was applied in precipitation time series to remove any autocorrelation before trend analysis [43-46], as autocorrelation affects the trend results. Autocorrelation values were calculated with a 95% confidence interval for precipitation data. The flow chart of the data pre-processing, methodology, and analysis is shown in Figure 2. It should be noted that the datasets used in the study have limitations in terms of spatial scales. The area did not have enough ground-based observations over the whole region with a uniform distribution, while it only covers NP, which may not be representative of precipitation trends in other regions. The numbers of meteorological stations in the sub-regions I–III are 11, 10, and 4, respectively (Table 2). The locations of each homogenous region in Pakistan are R-I (Gilgit-Baltistan and Chitral region, Upper Indus Basin and Chitral River Basin, Hindukush-Karakoram-Himalaya), R-II (Kakul-Cherat Hills, Swat Valley, Margalla Hills, Azad Jammu and Kashmir, Jhelum River Basin, Southwestern Himalaya), and R-III (Central KPK, southern parts of Kabul River Basin).

Table 2. Distribution of major regions and number of metrological stations in different climate zone of Pakistan

Region	Characteristics	Major regions	Stations
I	Semi-arid	Gilgit-Baltistan and Chitral region, Upper Indus Basin and Chitral River Basin, Hindukush-Karakoram-Himalaya	11
II	Humid	Kakul-Cherat Hills, Swat Valley, Margalla Hills, Azad Jammu and Kashmir, Jhelum River Basin, South western Himalaya	10
III	Humid	Central KPK, southern parts of Kabul River Basin	4

3.2. Mann−Kendall test and Sen's Slop Estimator

The non-parametric Mann-Kendall (MK) test is a commonly used test to identify trends in various time series because it is unaffected by the normal distribution of data time series and outliers [30,47-51]. The two hypotheses (null and alternative) were in this test identify the trend direction. The null hypothesis shows no trend in the time series, while the alternative indicates an increasing or decreasing trend. The determined Z value of this test follows the normal distribution with a variance average (0, 1) used to detect trend significance. So, according to this, an increasing trend was shown by $Z>0$, and vice versa [52-54]. In addition, Sen's slope estimator (SSE) determined the magnitude of the precipitation time series trend by a simple non-parametric procedure [43,55,56].

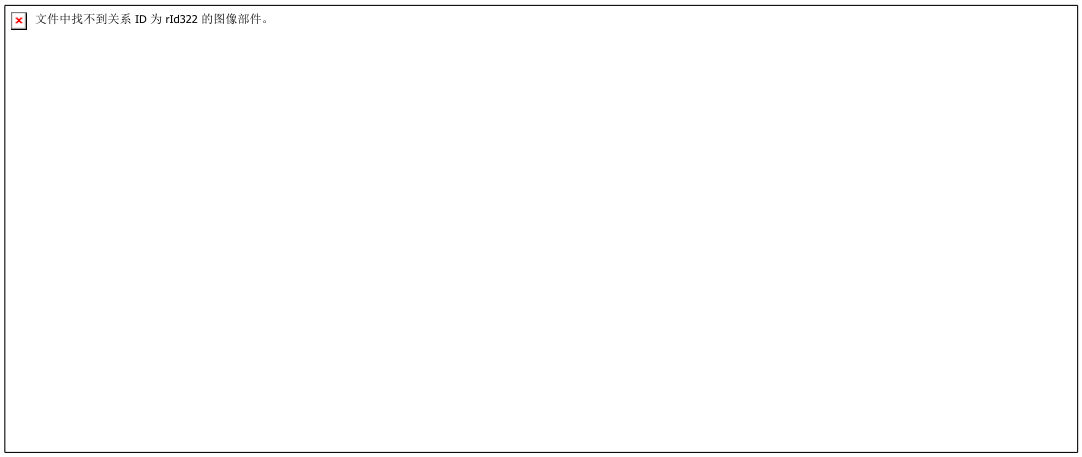

Figure 2. Flow chart of the data pre-processing, methodology, and analysis used.

3.3. The Sequential Mann-Kendall test (SQMK) Test

Sneyers introduced the SQMK test to analyze the significant change points in long-term time series [57-62]. The abrupt change in the trend is analyzed by the forward (SF) and backward (SB) sequential series. SF has sequential behavior, which changes around zero because SF is a standardized variable with a zero mean and unit standard deviation. In addition, it has the exact nature of Z values that start from the first point of the time series to the last point of the time series. On the other hand, SB is opposite to Z values as it moves from the last point to the start point of the time series [63,64]. In this study, we have chosen a 5% significance level. A negative trend shows when both SF and SB have decreasing values; on the other side, a positive trend shows when SF and SB have increasing values [65]. SF and SB intersect at a specific point; it describes a major abrupt change in that year in the time series [20].

3.4. Cluster Analysis

The use of clustering algorithms provides for the efficient division of big data sets into homogeneous clusters by acquiring knowledge [66,67]. The k-means cluster algorithm approach described by [67] carries out the following fundamental steps: (a) the procedure first establishes the centers of the K number of clusters and then each variable is assigned to the closest cluster center using only a similarity metric. (b) After assigning each parameter to a cluster as input data, all groups are recalculated for cluster centers. (c) The factors may be distributed among different clusters depending on where the new cluster centers are located. The "distance measure" is used to determine the

correlations of variables to cluster centers, and this strategy is continued until there is no modification in the cluster centers [68].

3.5. WTC Analysis

Wavelet coherence analysis (WTC) is a statistical tool used in signal processing and time-series analysis to examine the relationship between two signals as a function of time and frequency [69]. WTC involves using wavelet transforms, mathematical tools that can decompose signals into their frequency components and provide information on the power and phase of each frequency component. It transforms the two signals and then calculates their coherence at each frequency and time point [70]. The coherence value ranges from 0–1, where zero indicates no relationship between the two signals, and one indicates a perfect linear relationship between the two signals. WTC has applications in various fields, including neuroscience, environmental science, and economics [71]. Recently, Hussain et al. (69) analyzed the cross-correlation between precipitation series and large-scale climate indices using the WTC. The extent of a linear association in the time and frequency domain is assessed using this correlation coefficient, which is localized in the time and frequency domain [72]. The Monte Carlo approach calculates the significance level in WTC, and the cone of influence is used to calculate the significance level [73]. WTC displays the 95% confidence levels corresponding to the pink noise and draws attention to the significant coherence even though the common power of both variables is low.

Table 3. Mean seasonal and annual precipitation in different sub-regions of northern Pakistan.

	Winter	Spring	Summer	Autumn	Annual
R-I	48.42	103.75	47.68	28.80	229.54
R-II	259.59	324.80	556.88	178.25	1320.57
R-III	128.05	212.37	232.67	89.99	664.81
NP	166.48	237.06	308.63	110.52	823.80

4. Results

4.1. Climatology

The spatial distribution of the mean seasonal and annual precipitation in the different regions of NP is shown in Figure 3, while the sub-regional amounts are presented in Table 3. The results depict that the stations located in R-II received the highest mean precipitation annually, while stations in R-I received less precipitation than annually. The stations located in R-III received high annual precipitation but the precipitation amount is limited in autumn. NP's observed mean annual precipitation is 823 mm (Table 3). Annual and summer mean precipitation in R-II is 1320 mm and 556 mm, respectively. However, winter, spring, and autumn have below 350 mm of precipitation. Among all regions, R-II received the highest precipitation at seasonal and annual scales, followed by R-III and R-I (Table 3 and Figure 3). The amount of seasonal and annual precipitation is below 250 and 700 mm in R-I and III, respectively. Overall, maximum precipitation is obvious in summer, followed by spring and winter (Table 3).

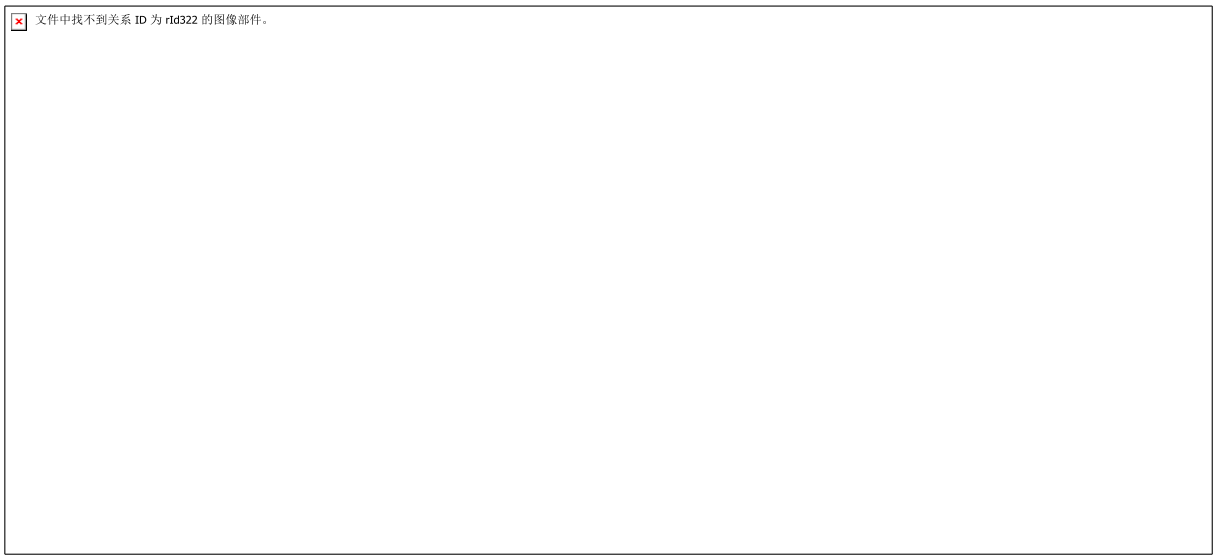

Figure 3. Spatial distribution of mean seasonal and annual precipitation (mm/decade) in northern Pakistan.

Figure 4. Spatial distribution of Mann-Kendall and Sen's seasonal and annual precipitation trends in northern Pakistan.

4.2. Spatiotemporal trends

The spatial distribution of MK and SSE trends for seasonal and annual precipitation in NP are shown in Figure 4, whereas regional trends during 1960–2016 are presented in Table 4. It is worth mentioning that the station density in the NP is very sparsely distributed and the number of stations with long-term observed datasets is very limited. Therefore, we have also used ERA-5 reanalysis precipitation data to supplement the observed dataset in reproducing the spatial distribution of precipitation in the whole region. The spatial trend of ERA-5 reanalysis datasets in NP is presented in Figure 5.

Winter precipitation shows an increasing (decreasing) trend at 13 (12) stations (Figure 4), whereas ERA-5 also displayed similar results; the southern and eastern region in NP Pakistan shows increasing trends while decreasing in the remaining sites (Figure 5). The lowest negative slopes were observed in stations of R-II; however, Naltar, Khunjerab, and Ziarat observed significant increasing trends. Most of the stations in R-II displayed negative trends (Figure 4). Winter precipitation in NP shows mixed trends, whereas increasing trends are observed in the R-I and III at a rate of 0.38 and 0.57 mm/decade, respectively. During the study period (1960–2016), R-II and NP kept

decreasing trends at −0.34 and −0.55 mm/decade, respectively (Table 4). In spring, the negative trend is evident over the whole NP with a significant decreasing trend in Astor (Figure 4). Spring precipitation is decreasing in R-I, II, and NP at the rates of −0.15, −0.40, and −0.75 mm/decade, respectively, while only an increase is observed in R-III during the study period (Table 4). The observed results agree with the ERA-5 reanalysis trends (Figure 5), as the region indicates a decreasing trend. In summer, the positive trends are obvious over R-I and R-III, while most stations in R-II exhibited negative trends (Figure 4), whereas summer precipitation is decreasing in R-II and III, while an increasing trend is obvious in R-I as observed in ERA-5 datasets (Figure 5). R-I and III exhibited significant positive trends at the rates of 0.39 and 1.64 mm/decade, respectively, whereas R-II and NP observed negative trends (Table 4). A mixture of positive and negative trends from 1960 to 2016 is evident in autumn.

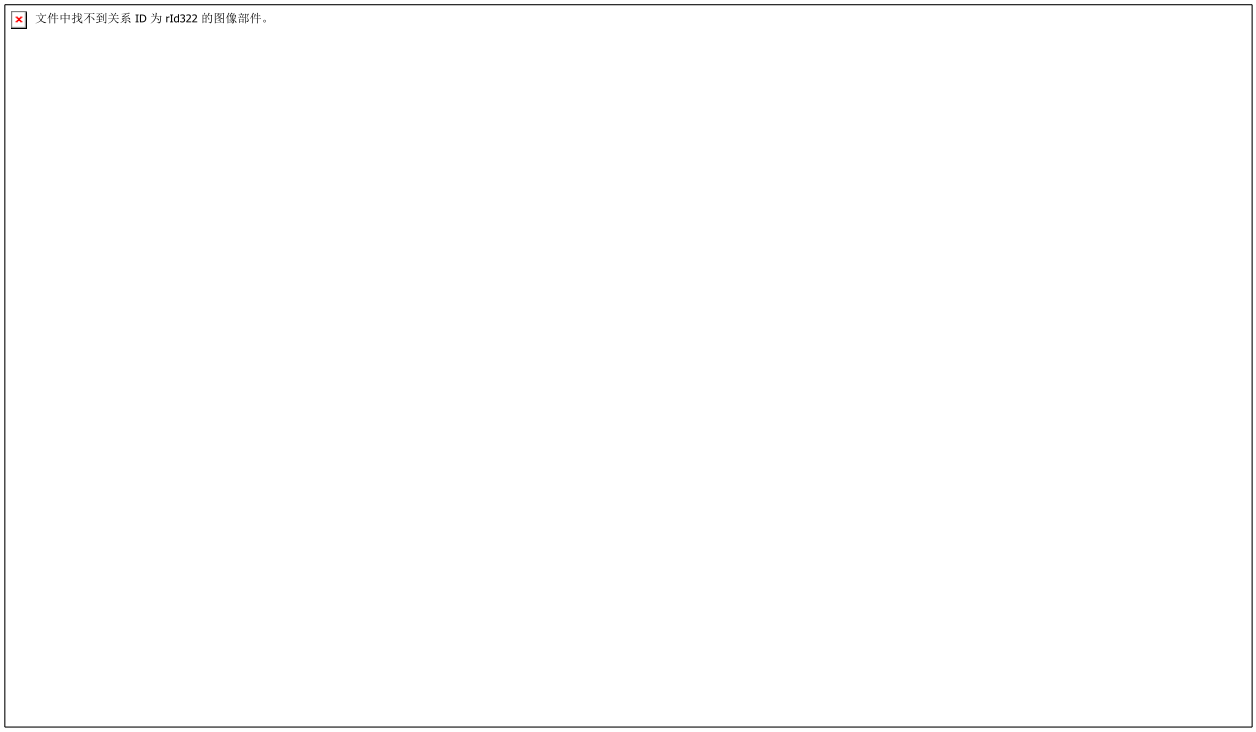

Figure 5. Spatial distribution of (a) winter, (b) spring, (c) summer, (d) autumn, and (e) annual precipitation trends with ERA-5 reanalysis datasets in northern Pakistan.

Autumn shows an increasing (decreasing) trend at 16 (08) stations (Figure 4), whereas increasing trends are more dominant, as observed in ERA-5 datasets in the whole region (Figure 5). Such increasing trends are more dominant in R-II, II, and in western parts of R-I. In R-I, most stations show positive trends; in R-III, all stations exhibit positive trends. According to the MK outcomes, Darosh and Murree witnessed significant negative trends, while Peshawar, Risalpur, Kakul, Skardu, and Gupis showed significant positive trends (Figure 4). All three sub-regions prevailed positive trends in autumn from 1960 to 2016 (Table 4). Most stations in R-I and III observed increasing trends while decreasing in R-II for annual precipitation (Figure 4). However, increasing trends are more prominent in R-I, whereas decreasing trends are obvious in R-II and III, as observed in the ERA-5 reanalysis results. Moreover, R-I and III observed significant increasing trends in annual precipitation at a rate of 1.05 and 3.95 mm/decade, respectively, and decreasing trend in R-II and NP during 1960–2016 (Table 4). Overall, the trends for observed data and ERA-5 reanalysis datasets are almost similar in winter, spring, and autumn; however, some disagreement is observed in both datasets in summer and annual precipitation trends in NP. The region is known for its complex topography, which can lead to significant orographic effects on precipitation patterns, particularly during the summer monsoon, whereas variations in atmospheric circulation patterns, such as the strength and position of the westerly jet stream, may also influence precipitation patterns in the region [74]. The disagreement

between observed data and ERA-5 reanalysis datasets in the NP could be due to the complex topography of the region, which can lead to significant orographic effects on precipitation patterns [75]. Additionally, the influence of the South Asian Summer Monsoon and variations in vegetation cover and atmospheric circulation patterns may also contribute to discrepancies between the datasets, and due to the combination of factors in NP [76].

Table 4. Mann-Kendall and Sen's slope trends for seasonal and annual precipitation (mm/decade) in different sub-regions of northern Pakistan. Bold indicates 5% significance levels.

Period		Winter	Spring	Summer	Autumn	Annual
1960−1988	R-I	−0.11	−0.52	**0.88**	0.37	1.53
	R-II	−0.13	1.35	1.19	0.43	5.94
	R-III	−0.98	−1.69	0.84	**−1.02**	−3.35
	NP	−0.18	0.38	2.07	0.24	3.33
1989−2016	R-I	−0.28	−0.87	−0.58	0.20	−0.45
	R-II	−5.24	−3.14	−2.92	−0.21	−7.90
	R-III	0.08	2.80	**5.49**	2.24	**12.55**
	NP	−2.76	−1.19	−0.54	0.43	−1.91
1960−2016	R-I	0.38	−0.15	**0.39**	0.12	**1.05**
	R-II	−0.34	−0.40	−1	0.00	−1.14
	R-III	0.57	0.20	**1.64**	0.63	**3.95**
	NP	−0.55	−0.75	−1.66	−0.19	−2.86

For a more detailed and systematic analysis, the whole period is divided into two sub-periods, i.e., 1960−1988 and 1989−2016 (Table 4). In winter, precipitation in R-I, II, II, and NP decreased during 1960−1988, which is also prominent in the second period, except for an increase in R-III with 0.08 mm/decade. For spring, precipitation increased during 1960−1988 in NP while decreasing during 1989−2016; however, mixed trends prevailed in the sub-regions in both periods. Summer precipitation increases in the first period in all sub-regions and NP, while a decrease is observed in R-I, II, and NP. Autumn shows steadily increasing trends in both periods in all sub-regions. Furthermore, annual precipitation in NP increased in the first period at a rate of 3.33 mm/decade, decreasing in the second period at a rate of −1.91 mm/decade, respectively.

4.3. Temporal variations

Anomalies for annual and seasonal precipitation are shown in Figure 6. No clear trends are observed in NP for winter precipitation until the mid-1980s, but an increasing trend is apparent afterward. The increasing trend is also prominent annually, with the anomalies dominated by positive values from the mid-1980s onwards. The anomaly values keep changing for spring, summer, and autumn without any clear trend.

The SQMK analysis was further employed to assess the abrupt shifts in seasonal and annual precipitation in NP, and the results are shown in Figure 7. In winter, abrupt shifts were observed between 1961 and 1985, while a rapid upward shift is evident after the min-1980s until 2010. Significant abrupt changes in spring are detected during 1967–1980. A sharp decreasing shift was observed in 1967. An increasing trend is observed in 1980, while a downward trend is evident from mid-2000 onwards. In summer, there is a clear increasing trend until 1975; however, a decreasing trend is noticeable afterward. Similarly, autumn showed an increasing trend until 2010. Annual precipitation shows an increasing trend from the mid-1970s onwards; however, a major downward trend is obvious after 2000.

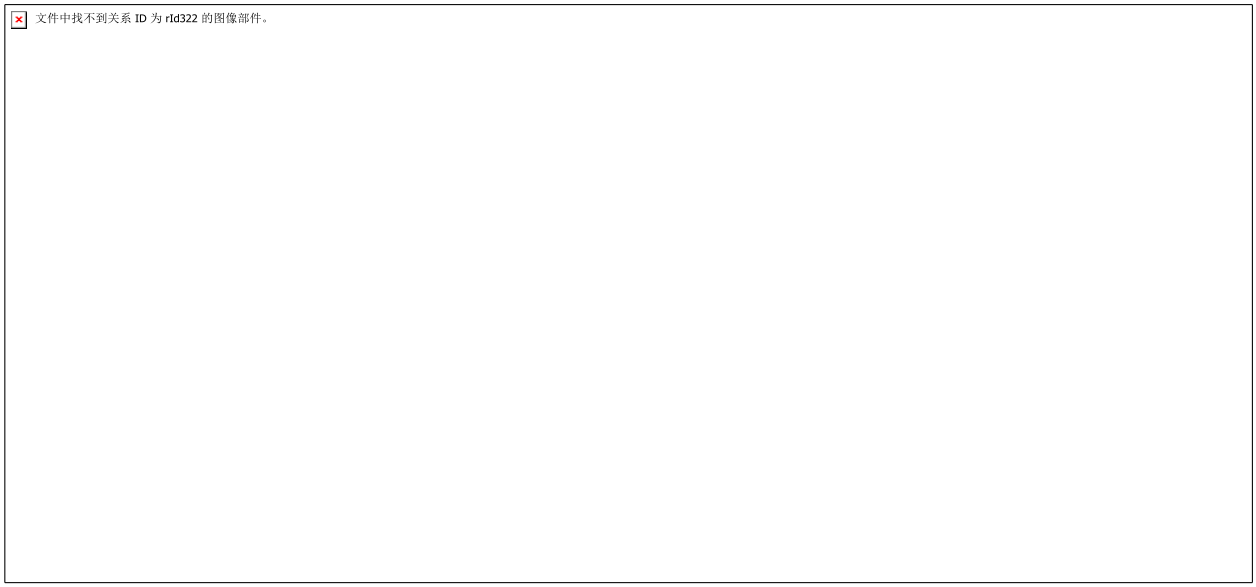

Figure 6. Seasonal and annual time-series anomalies relative to 1961−1990 mean values for seasonal and annual precipitation in northern Pakistan. The smooth line indicates a five-year moving average.

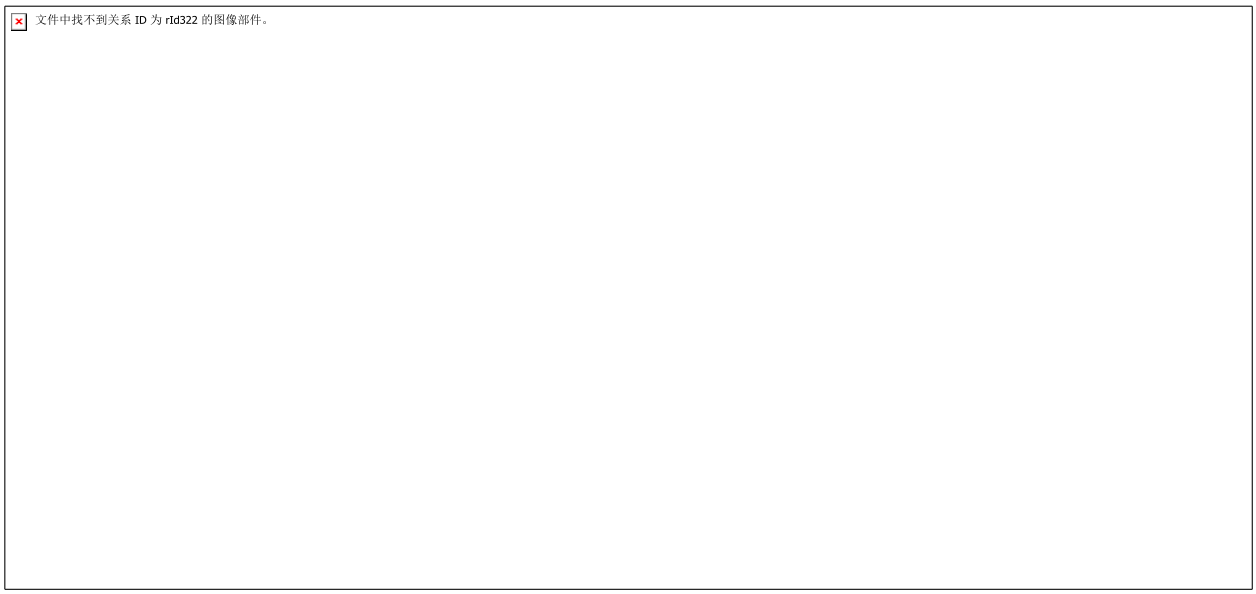

Figure 7. Temporal changes of Z value based on the Mann-Kendall test for seasonal and annual precipitation in northern Pakistan.

The temporal trends in annual precipitation are assessed over six different elevation zones in NP (Figure 8). The various elevation zones are <500 m, 500–1000 m, 1000–1500 m, 1500–2000 m, 2000–2500 m, and 2500–5000 m. The annual precipitation shows an increasing trend in<500 m, 100–1500 m, 1500–2000 m, 2000–2500 m, and 2500–5000 m, whereas a decreasing trend is observed in 500–1000 m.

Figure 8. Temporal trends of annual precipitation in northern Pakistan. The blue line indicates linear trends, while the red line is the five-year moving mean.

4.4. Coherence of precipitation with teleconnections

Figure 9 displays the WTC results for the AMO, AO, NAO, ENSO, IOD, and PDO over NP from 1960 to 2016. The pink color shows the percent area of significant coherence (PASC) relative the total areas, and black circles with pink colors show high coherence. In this study, the WTC analysis is preferred over other methods because it indicates the coherences over time and space [65]. However, the traditional correlation or regression analysis can only give one value with the degree of linear correlation between two variables. The WTC indicates the temporal signals of various teleconnections with the regional precipitation at interannual, decadal, and interdecadal scales. Significant interdecadal coherences are evident with AO and PDO from 128 months and above, whereas most significant interannual coherences in ENSO are found at 16–128 months (Figure 9). Moreover, AO, ENSO, and IOD witnessed higher coherence with precipitation in NP, whereas AMO, NAO, and PDO observed fewer coherences. The observed findings of AO, IOD, PDO, and ENSO agree with the results reported by [69] in the monsoon region of Pakistan.

Changes in precipitation on a monthly time scale differ from those on seasonal and yearly scales, as different indices have different degrees of effect throughout multiple seasons. For instance, the dominating factors that impact many regions of the planet are the large-scale modes in the AO, NAO, ENSO, and PDO, each operating at a very different time. Therefore, we have further explored the precipitation association on seasonal and annual scales using regression analysis to complement the wavelet coherence. Table 5 shows the regression of oceanic indices with regionally averaged seasonal and annual precipitation. The regression values of 3.40 and 1.97 suggest a linear association of winter precipitation with AO and ENSO, respectively. While a negative association of precipitation with NAO, IOD, and PDO indices at the rates of –2.28, –2.40, and –1.08, respectively. The regression coefficients of 1.86 and 0.08 show a linear spring precipitation association with ENSO and PDO, respectively. On the other hand, a negative association of precipitation with AO, NAO, and IOD is evident, having –0.21, –0.32, and –4.40 regression, respectively. The regression values of 1.27, 0.68, and 1.11 suggest a linear association of summer precipitation with AO, IOD, and PDO, respectively, while a negative association between NAO and ENSO at –1.12 and –1.33, respectively. On the annual scale, a positive relationship with AO, ENSO, and PDO at 3.34, 2.19, and 0.63, respectively, while a negative relationship with NAO (–1.28) and IOD (–6.10) is observed. Overall, winter

precipitation had higher linear regression with AO, and spring with ENSO, while AO, IOD, and PDO had higher influence during summer, whereas AO and ENSO are dominant at annual time scales.

5. Discussion

Due to the frequent and intense climatic events, sensitive places are anticipated to be exposed exponentially over the globe to floods and droughts, which can raise associated risk and susceptibility [77]. For most of Pakistan, the northern sub-Himalayan region is the country's primary water source and is highly sensitive to climate change. Pakistan's hydrology and water security may be severely affected by changes in precipitation in NP. The non-parametric MK, SSE, SQMK, and WTC analysis are used to observe the trends and precipitation relation with oceanic indices.

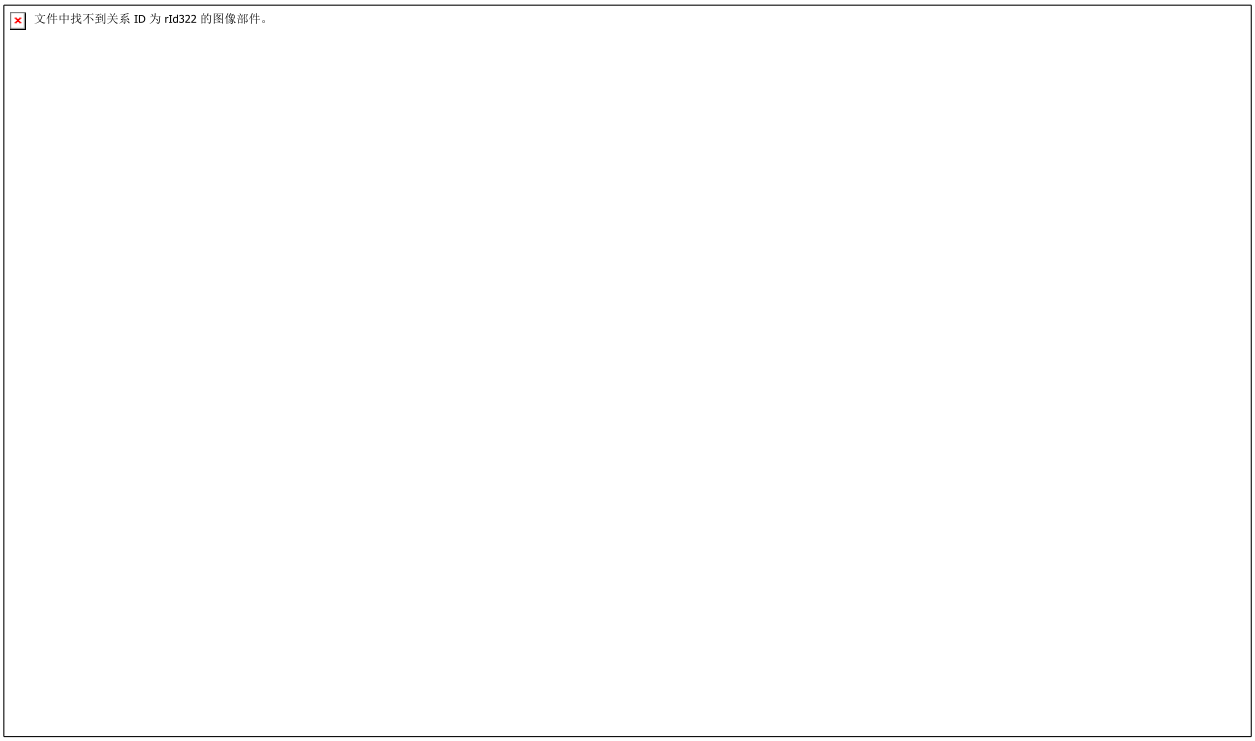

Figure 9. Wavelet coherence between monthly precipitation over northern Pakistan with (a) AMO, (b) AO, (c) NAO, (d) ENSO, (e) IOD, (f) PDO. Right-pointing arrows indicate that the two signals are in phase, while the left is for antiphase signals. Thick contours denote 5% significance levels against pink noise.

Table 5. Regression of oceanic indices with regionally averaged seasonal and annual precipitation.

Season	Index	Estimate	SE	p-value
Winter	AO	3.40	1.08	0.002
	NAO	–2.28	0.77	0.004
	ENSO	1.97	0.72	0.008
	IOD	–2.40	1.71	0.16
	PDO	–1.08	0.45	0.02
Spring	AO	–0.21	1.22	0.85
	NAO	–0.32	0.87	0.71
	ENSO	1.86	0.81	0.02

	IOD	–4.40	1.92	0.02
	PDO	0.08	0.52	0.87
Summer	AO	1.27	0.78	0.10
	NAO	–1.12	0.56	0.04
	ENSO	–1.33	0.52	0.01
	IOD	0.68	1.23	0.58
	PDO	1.11	0.33	0.001
Annual	AO	3.34	1.54	0.03
	NAO	–1.28	1.10	0.24
	ENSO	2.19	1.02	0.037
	IOD	–6.10	2.43	0.01
	PDO	0.63	0.65	0.33

Results infer maximum precipitation during annual and summer (Figure 3, Table 3), which agrees with numerous studies [23,78]. The spatial and temporal trends for seasonal and annual precipitation over different sub-climatic regions show that the trend's magnitude varies from region to region and station to station [51]. Annual and summer mean precipitation in R-II is 1320 and 556 mm, respectively. Results show that annual and summer mean precipitation is highest, especially in R-II [51,79]. The seasonal and annual precipitation trends decreased in NP during 1960−2016. While summer and annual precipitation significantly increased in R-I and R-III [30], R-II and III are influenced by monsoons and westerlies [20].

In two sub-periods, 1960−1988 and 1989−2016, Precipitation in R-I, II, III, and NP declined in the winter from 1960 to 1988. This trend is still apparent in the second period [30], except for an increase in R-III. Precipitation in spring increased in NP in both periods; nevertheless, mix trends dominate the sub-regions [80]. All sub-regions and NP are experiencing increased summer precipitation [69] during the first period. Additionally, the annual precipitation in NP changes with time [81], increasing in the first sub-period and decreasing in the second sub-period of the study period (Table 4). These results are consistent with the findings of [81-83]. It has been explained earlier that there has been a noticeable increase in the amount of precipitation during the South Asian summer monsoon, sometimes with wet extremes, which is mostly due to the East Asian summer monsoon's penetration and a western disturbance over the country's northern mountainous regions [84]. There are indicators that strong and widespread human activity in Asia has begun to disrupt the monsoon season [30,85], while La Nina's influence supports high summer monsoon rainfall over South Asia [86]. Furthermore, the monsoon may be shifting west, carrying more moisture and producing additional rains and extreme events across Pakistan [82]. Summer and annual precipitation in R-III are significantly increasing during 1960−2016. These findings are consistent with the results of [87], whereas [88] and [89] explained and attributed it to the projected increase in South Asian summer monsoon precipitation status under enhanced greenhouse gas emission scenarios.

The anomaly values fluctuate throughout spring, summer, and autumn with no discernible pattern [90]. The rising precipitation shows the region's monsoons are getting stronger. The monsoons are becoming less frequent but more potent in some parts of South Asia, increasing the likelihood of catastrophic weather events there [20]. Until the middle of the 1980s, there were often no discernible patterns in the amount of winter precipitation in NP [91], but from 1985 to 2005, there was a distinct upward trend. Such growing tendencies are also present in annual data,

with positive values dominating the anomalies from the middle of the 1980s to 2016. Similar results are consistent with [82,83,92].

Winter time significant shifts were seen between 1961 and 1985 [93], and from the mid-1980s to 2010, there has been a rapidly increasing shift. Between 1967 and 1980, spring underwent its most significant dramatic changes. In 1967, a sudden diminishing shift was noticed (Figure 6). While there was an upward tendency in 1980, there has been a downward trend since about mid-2000. Until 1975, there was a noticeable upward trend for the summer but a definite downward trend [94]. The same is true for the autumn precipitation trend in 2010. From the middle of the 1970s onward, annual precipitation indicates an increasing trend [83]; however, after 2000, a significant declining trend is evident. These results are with good agreements of [51,95].

Throughout the study period, various trends were visible in the annual precipitation at various altitudes. Past studies show a positive correlation between precipitation and elevation [96,97]. The annual precipitation increases in the altitude zones of 500 m, 100–1500 m, 1500–2000 m, 2000–2500 m, and 250–5000 m. The deepening of the land-sea thermal contrast, which enhances moisture flux transfer from the ocean toward the land, may cause an increasing precipitation trend. In contrast, a declining tendency was seen in the 500–1000 m elevation range. Between 1960 and 2016, significant interdecadal coherences with AO and PDO spanning from 128 months and above. The ENSO's most notable interannual coherences were during 16–128 months. In contrast to AMO, NAO, and PDO, AO, ENSO, and IOD generally showed higher coherences with precipitation in NP [69,98].

Studies found a considerable rise in maximum and minimum temperatures over Pakistan between 1980 and 2016, which might significantly affect precipitation [16]. According to Hussain and Lee [99], widespread urbanization and a sharp rise in population in the middle and upper Punjab, particularly after the 1980s, are two potential causes of rising precipitation. Such variations may be brought on by mechanical variability induced by increased surface lumpiness and sensible heat from the warm metropolitan air. Additionally, an increase in precipitation in South Asia is due to the vapor transfer from the Arabian Sea and the Bay of Bengal [100,101]. A recent trend towards a lesser monsoonal effect is shown by a change in long-term summer wetting to drying between 1995–2012 [102]. A decrease in the north-south sea surface temperature gradient across the North Indian Ocean and the monsoon circulation over Pakistan is to blame for the dip in rainfall activity [103,104].

Moreover, de Oliveira-Júnior et al. [105] discovered that ENSO greatly impacts Pakistan's yearly precipitation. They also studied how AMO and PDO affected precipitation variability in the UIB. Attada et al. [106] revealed strong associations between the mean temperature and the global teleconnections with NAO and ENSO during the spring, as how the NAO might affect certain monsoon months, particularly August. In the southern regions of Central Asia, winter precipitation is significantly influenced by the NAO and ENSO. The Indian monsoon, which controls the southern portion of Central Asia, can be severely impacted by the warm phase of the AMO concurrently [107]. According to another study, the NAO and ENSO precipitation signals in Central Southwest Asia are mostly related to an intensification of westerlies that move eastward across the territory of Central Southwest Asia (including northern Pakistan) during the positive NAO and the warm ENSO phases [108].

6. Conclusion

The present study used the non-parametric MK, SSE, SQMK, cluster analysis, and WTC analysis to observe seasonal and annual precipitation trends, variability, and teleconnections. Based on the current study's findings and detailed literature, there is a need to the assessment of the influencing mechanism systematically and comprehensively.

In the spatial distribution of mean seasonal and annual precipitation, all regions received the highest precipitation annually. R-II received the highest precipitation at seasonal and annual scales, followed by R-III and I. At the same time, R-I and III received seasonal and annual precipitation below 250 and 700 mm, respectively. Generally, maximum precipitation is observed in summer, followed by spring and winter. According to the MK and

SS, most stations in R-I and III observed increasing trends, while decreasing in R-II was observed for annual precipitation. Moreover, R-I and III observed significant increasing trends in annual precipitation and decreasing in R-II and NP during 1960–2016. Moreover, the spatial trends for observed data and ERA-5 reanalysis datasets are almost similar in winter, spring, and autumn; however, some disagreements are observed in both datasets in summer and annual precipitation trends in NP.

The whole period is divided into two sub-periods, which are 1960−1988 and 1989−2016. In winter, precipitation in R-I, II, III, and NP decreased during 1960−1988, which is also prominent in the second period. For spring, precipitation increased during the first period in NP while decreasing during the second time scale; however, mixed trends prevail in both time scales. Summer precipitation increases in the first period in all sub-regions and NP, while a decrease is observed in R-I, II, and NP. Autumn shows steadily increasing trends in both periods in all sub-regions. Furthermore, annual precipitation in NP increased in the first period and decreased in the second.

In temporal variations, no clear trend is observed in all seasons except in annual and winter. An increasing trend is evident in annual and winter during 1985–2016 and 1985–2005, respectively. According to the SQMK, most trends increased in all seasons until 1980 and a downward shift after 2010.

The temporal trends in annual precipitation are assessed over six elevations. The annual precipitation shows an increasing trend in <500 m, 100–1500 m, 1500–2000 m, 2000–2500 m, and 2500–5000 m, whereas the decreasing trend is observed in 500–1000 m. According to WTC, AO, ENSO, and IOD witnessed higher coherence with precipitation in NP, whereas AMO, NAO, and PDO observed fewer coherences.

Winter precipitation has a higher linear regression with AO and spring with ENSO, while AO, IOD, and PDO have higher influence on summer precipitation, whereas AO and ENSO are dominant at annual time scale.

Author contributions:

Conceptualization: AH; Methodology: AH, and IH; Formal analysis and investigation: AR and AH; Writing - original draft preparation: AR and AH; Writing - review and editing AR, AH, WU, HA, and SU, Funding: JZ and JC.

Funding Information: The National Natural Science Foundation of China, Grant No. 31870707.

Institutional Review Board Statement: Not applicable.

Informed Consent Statement: Not applicable.

Acknowledgement: The authors acknowledge the Pakistan Meteorology Department for providing precipitation data for this research. The ERA5-Reanalysis data can be downloaded from the website: https://cds.climate.copernicus.eu/cdsapp#!/search? type=dataset.

Conflicts of Interest: The authors declare no conflict of interest.

References

1. Perotti, E.; Huguenin-Elie, O.; Meisser, M.; Dubois, S.; Probo, M.; Mariotte, P. Climatic, soil, and vegetation drivers of forage yield and quality differ across the first three growth cycles of intensively managed permanent grasslands. *Eur. J. Agron.* **2021**, *122*, 126194.

2. Palmer, M.; and Ruhi, A. Linkages between flow regime, biota, and ecosystem processes: Implications for river restoration. *Sci.* **2019**, *365*.

3. Li, X.; Zhang, K.; Gu, P.; Feng, H.; Yin, Y.; Chen, W.; Cheng, B. Changes in precipitation extremes in the Yangtze River Basin during 1960–2019 and the association with global warming, ENSO, and local effects. *Sci.Tot. Environ*. **2021**, *760*, 144244.

4. Hrudya, P.; Varikoden, H.; Vishnu, R. A review on the Indian summer monsoon rainfall, variability and its association with ENSO and IOD. *Meteor. Atmos. Phy.* **2021**, *133*, 1-14.

5. Papalexiou, S.M.; and Montanari, A. Global and regional increase of precipitation extremes under global warming. *Wat.*

Resou. Res. **2019**, *55*, 4901-4914.

6. Reichle, R.H.; Koster, R.D.; De Lannoy, G.J.; Forman, B.A.; Liu, Q.; Mahanama, S.P.; Touré, A. Assessment and enhancement of MERRA land surface hydrology estimates. *J. clim.* **2011**, *24*, 6322-6338.

7. Zhang, Y.; You, Q.; Ullah, S.; Chen, C.; Shen, L.; and Liu, Z. Substantial increase in abrupt shifts between drought and flood events in China based on observations and model simulations. *Sci. Tot. Environ.* **2023**, 162822.

8. Yu, Y.; You, Q.; Zuo, Z.; Zhang, Y.; Cai, Z.; Li, W.; Jiang, Z.; Ullah, S.; Tang, X.; Zhang, R. Compound climate extremes in China: Trends, causes, and projections. *Atmos. Res.* **2023**, 106675.

9. Tuel, A.; and Martius, O. A global perspective on the sub-seasonal clustering of precipitation extremes. *Weath. clim. extr.* **2021**, *33*, 100348.

10. Rivera-ferre, M.; Di Masso, M.; Vara, I.; Cuellar, M.; López-i-Gelats, F.; Bhatta, G.; Gallar, D. Traditional agricultural knowledge in land management: the potential contributions of ethnographic research to climate change adaptation in India, Bangladesh, Nepal, and Pakistan. *Clim. Develop.* **2021**, 1-18.

11. Waqas, H.; Lu, L.; Tariq, A.; Li, Q.; Baqa, M.F.; Xing, J.; Sajjad, A. Flash Flood Susceptibility Assessment and Zonation Using an Integrating Analytic Hierarchy Process and Frequency Ratio Model for the Chitral District, Khyber Pakhtunkhwa, Pakistan. *Wat.* **2021**, *13*, 1650.

12. Eckstein, D.; Künzel, V.; and Schäfer, L. Global Climate Risk Index 2021. *Who Suffers Most from Extreme Weather Events* **2021**, 2000-2019.

13. Abbas, A.; Bhatti, A.S.; Ullah, S.; Ullah, W.; Waseem, M.; Zhao, C.; Dou, X.; and Ali, G. Projection of precipitation extremes over South Asia from CMIP6 GCMs. *J. Ari. Lan.* **2023**, 1-23.

14. Hu, P.; Sharifi, A.; Tahir, M.N.; Tariq, A.; Zhang, L.; Mumtaz, F.; and Shah, S.H.I.A. Evaluation of Vegetation Indices and Phenological Metrics Using Time-Series MODIS Data for Monitoring Vegetation Change in Punjab, Pakistan. *Wat.* **2021**, *13*, 2550.

15. Arshad, M.; Ma, X.; Yin, J.; Ullah, W.; Ali, G.; Ullah, S.; Liu, M.; Shahzaman, M.; Ullah, I. Evaluation of GPM-IMERG and TRMM-3B42 precipitation products over Pakistan. *Atmos. Res.* **2021**, *249*, 105341, doi:https://doi.org/10.1016/j.atmosres.2020.105341.

16. Ullah, W.; Wang, G.; Ali, G.; Tawia Hagan, D.F.; Bhatti, A.S.; Lou, D. Comparing multiple precipitation products against in-situ observations over different climate regions of Pakistan. *Rem. Sens.* **2019**, *11*, 628.

17. Lau, W.K.; and Kim, K.-M. The 2010 Pakistan flood and Russian heat wave: Teleconnection of hydrometeorological extremes. *J. Hydromet.* **2012**, *13*, 392-403.

18. Wu, H.; Guo, B.; Fan, J.; Yang, F.; Han, B.; Wei, C.; Lu, Y.; Zang, W.; Zhen, X.; Meng, C. A novel remote sensing ecological vulnerability index on large scale: A case study of the China-Pakistan Economic Corridor region. *Ecologic. Indic.* **2021**, *129*, 107955, doi:https://doi.org/10.1016/j.ecolind.2021.107955.

19. Heike Hartmann, H.B. Trends in Extreme Precipitation Events in the Indus River Basin and Flooding in Pakistan. *Atmos. Oce.* **2013**, *52*, 77-91, doi:https://doi.org/10.1080/07055900.2013.859124.

20. Hussain, A.; Cao, J.; Hussain, I.; Begum, S.; Akhtar, M.; Wu, X.; Guan, Y.; and Zhou, J. Observed Trends and Variability of Temperature and Precipitation and Their Global Teleconnections in the Upper Indus Basin, Hindukush-Karakoram-Himalaya. *Atmos.* **2021**, *12*, 973.

21. Adnan, S.; Ullah, K.; Gao, S.; Khosa, A.H.; Wang, Z. Shifting of agro□climatic zones, their drought vulnerability, and precipitation and temperature trends in Pakistan. *Int.l J.Clim.* **2017**, *37*, 529-543.

22. Gadiwala, M.S.; and Burke, F. Climate change and precipitation in Pakistan-a meteorological prospect. *Int.l J. Econ.Environ. Geo.* **2019**, 10-15.

23. Ahmad, I.; Tang, D.; Wang, T.; Wang, M.; and Wagan, B. Precipitation trends over time using Mann-Kendall and spearman's rho tests in swat river basin, Pakistan. *Advan. Met.* **2015**, *2015*.

24. Iqbal, M.; and Hussain, A. Variability, trends, and teleconnections of observed precipitation over Pakistan. *Theor.Appl. Clim.* **2018**, *134*, doi:10.1007/s00704-017-2296-1.

25. Afzal, M.; Haroon, M.; Rana, A.; Imran, A. Influence of north Atlantic oscillations and southern oscillations on winter precipitation of northern Pakistan. *Pak. J.Met.* **2013**.

26. Iftikhar, A.; Zhaobo R.A.; Weitao, D. Winter-Spring Precipitation Variability in Pakistan. *Americ. J. Clim. Chan*. **2015**, *4*, 115.

27. Zaman, M.; Ahmad, I.; Usman, M.; Saifullah, M.; Anjum, M.N.; Khan, M.I.; Uzair Qamar, M. Event-Based Time Distribution Patterns, Return Levels, and Their Trends of Extreme Precipitation across Indus Basin. *Wat*. **2020**, *12*, 3373.

28. Akhtar, M.; Zhao, Y.; Gao, G.; Gulzar, Q.; Hussain, A. Assessment of spatiotemporal variations of ecosystem service values and hotspots in a dryland: A case□study in Pakistan. *Lan. Degrad. Develop*. **2022**, *33*, 1383-1397.

29. Nawaz, Z.; Li, L.; Chen, G.; Guo, Y.; Wang, X.; Nawaz, N. Temporal and Spatial Characteristics of Precipitation and Temperature in Punjab, Pakistan. *Wat*. **2019**, *11*, 1916, doi:10.3390/w11091916.

30. Hussain, A.; Cao, J.; Ali, S.; Muhammad, S.; Ullah, W.; Hussain, I.; Akhtar, M.; Wu, X.; Guan, Y.; Zhou, J. Observed trends and variability of seasonal and annual precipitation in Pakistan during 1960–2016. *Int. J. Clim*. **2022**.

31. Bookhagen, B.; and Burbank, D.W. Toward a complete Himalayan hydrological budget: Spatiotemporal distribution of snowmelt and rainfall and their impact on river discharge. *J. Geophy. Res.: Ear. Surf*. **2010**, *115*, doi:https://doi.org/10.1029/2009JF001426.

32. Abbas, A.; Ullah, S.; Ullah, W.; Waseem, M.; Dou, X.; Zhao, C.; Karim, A.; Zhu, J.; Hagan, D.F.T.; Bhatti, A.S. Evaluation and projection of precipitation in Pakistan using the Coupled Model Intercomparison Project Phase 6 model simulations. *Int. J. Clim*. **2022**.

33. Khan, I.; Waqas, T.; Ullah, S. Precipitation variability and its trend detection for monitoring of drought hazard in northern mountainous region of Pakistan. *Arab. J. Geosci*. **2020**, *13*, 1-18.

34. Abbasi, A.M.; Shah, M.H.; Khan, M.A. Pakistan and Pakistani Himalayas. In *Wild Edible Vegetables of Lesser Himalayas*; Spring. **2015**, 1-18.

35. Black, M. The atlas of water: mapping the World's most critical resource; Univ of California Press: **2016**.

36. Rondhi, M.; Fatikhul Khasan, A.; Mori, Y.; Kondo, T. Assessing the role of the perceived impact of climate change on national adaptation policy: the case of rice farming in Indonesia. *Lan*. **2019**, 8, 81.

37. Hussain, A.; Ali, H.; Begum, F.; Hussain, A.; Khan, M.Z.; Guan, Y.; Zhou, J.; Hussain, K. Mapping of Soil Properties under Different Land Uses in Lesser Karakoram Range, Pakistan. *Pol. J. Environ. Stud*. **2021**, *30*.

38. Azam, A.; and Shafique, M. Agriculture in Pakistan and its Impact on Economy. *A Review. Inter. J. Adv. Sci. Technol* **2017**, *103*, 47-60.

39. Sharma, S.; Hamal, K.; Pokharel, B.; Fosu, B.; Wang, S.Y.S.; Gillies, R.R.; Aryal, D.; Shrestha, A.; Marahatta, S.; Hussain, A.; et al. Atypical forcing embedded in typical forcing leading to the extreme summer 2020 precipitation in Nepal. *Clim. Dyn*. **2023**, doi:10.1007/s00382-023-06777-9.

40. Bhatti, A.S.; Wang, G.; Ullah, W.; Ullah, S.; Fiifi Tawia Hagan, D.; Kwesi Nooni, I.; Lou, D.; Ullah, I. Trend in extreme precipitation indices based on long term in situ precipitation records over Pakistan. *Wat*. **2020**, *12*, 797.

41. Khalil, A. Inhomogeneity detection in the rainfall series for the Mae Klong River Basin, Thailand. *Appl. Wat. Sci*. **2021**, *11*, 1-11.

42. Ahmed, K.; Nawaz, N.; Khan, N.; Rasheed, B.; Baloch, A. Inhomogeneity detection in the precipitation series: case of arid province of Pakistan. *Environ. Develop.Sustain*. **2021**, *23*, 7176-7192.

43. Ray, S.; Das, S.S.; Mishra, P.; Al Khatib, A.M.G. Time series SARIMA Modelling and forecasting of monthly rainfall and temperature in the south Asian countries. *Ear. Sys.Environ*. **2021**, 1-16.

44. Mirdashtvan, M.; Najafinejad, A.; Malekian, A.; and Sa'doddin, A. Regional analysis of trend and non□stationarity of hydro□climatic time series in the Southern Alborz Region, Iran. *Int. J. Clim*. **2020**, *40*, 1979-1991.

45. Piles, M.; Muñoz-Marí, J.; Guerrero-Curieses, A.; Camps-Valls, G.; and Rojo-Álvarez, J.L. Autocorrelation Metrics to Estimate Soil Moisture Persistence From Satellite Time Series: Application to Semiarid Regions. *IEEE Tran. Geoscie. Rem. Sens*. **2021**.

46. Ullah, S.; You, Q.; Ali, A.; Ullah, W.; Jan, M.A.; Zhang, Y.; Xie, W.; Xie, X. Observed changes in maximum and minimum temperatures over China-Pakistan economic corridor during 1980–2016. *Atmos. res*. **2019**, *216*, 37-51.

47. Agbo, E.P.; Ekpo, C.M.; Edet, C.O. Analysis of the effects of meteorological parameters on radio refractivity, equivalent potential temperature and field strength via Mann-Kendall test. *Theor. Appl. Clim*. **2021**, *143*, 1437-1456.

48. Ashraf, M.S.; Ahmad, I.; Khan, N.M.; Zhang, F.; Bilal, A.; Guo, J. Streamflow Variations in Monthly, Seasonal, Annual and Extreme Values Using Mann-Kendall, Spearmen's Rho and Innovative Trend Analysis. *Wat. Res. Manag*. **2021**, *35*, 243-261.

49. Karami, S.; Hossein Hamzeh, N.; Sabzezari, H.; Lo Alizadeh, M. Investigation of trend analysis of the number of dust stormy days and aerosol concentration derived from satellite in Khuzestan province by using non-parametric Mann-Kendall test. *J. Clim. Res*. **2021**, *1399*, 91-103.

50. Kubiak-Wójcicka, K.; Pilarska, A.; Kamiński, D. The Analysis of Long-Term Trends in the Meteorological and Hydrological Drought Occurrences Using Non-Parametric Methods—Case Study of the Catchment of the Upper Noteć River (Central Poland). *Atmos*. **2021**, *12*, 1098.

51. Ullah, S.; You, Q.; Ullah, W.; Ali, A. Observed changes in precipitation in China-Pakistan economic corridor during 1980–2016. *Atmos. Res*. **2018**, *210*, 1-14.

52. Seenu, P.; and Jayakumar, K. Comparative study of innovative trend analysis technique with Mann-Kendall tests for extreme rainfall. *Arab. J.Geoscie*. **2021**, *14*, 1-15.

53. Mohsin, S.; and Lone, M. Trend analysis of reference evapotranspiration and identification of responsible factors in the Jhelum River Basin, Western Himalayas. *Mod.Ear. Sys. Environ*. **2021**, *7*, 523-535.

54. Baig, M.R.I.; Naikoo, M.W.; Ansari, A.H.; Ahmad, S.; Rahman, A. Spatio-temporal analysis of precipitation pattern and trend using standardized precipitation index and Mann–Kendall test in coastal Andhra Pradesh. *Modeling Ear. Sys.Environ*. **2021**, 1-20.

55. Asgher, S.; Ahmad, M.; Kumar, N.; Kumari, M. Trend Analysis of Temperature and Rainfall using Mann Kendall Test and Sen's Slope Estimator in Bhaderwah Tehsil of Doda District. **2021**.

56. Aditya, F.; Gusmayanti, E.; Sudrajat, J. Rainfall trend analysis using Mann-Kendall and Sen's slope estimator test in West Kalimantan. In Proceedings of the IOP Conference Series: Ear. Environ. Sci., **2021**, 012006.

57. AlSubih, M.; Kumari, M.; Mallick, J.; Ramakrishnan, R.; Islam, S.; Singh, C.K. Time series trend analysis of rainfall in last five decades and its quantification in Aseer Region of Saudi Arabia. *Arab. J. Geoscie*. **2021**, *14*, 1-15.

58. Gupta, N.; Banerjee, A.; Gupta, S.K. Spatio-temporal trend analysis of climatic variables over Jharkhand, India. *Ear. Sys. Environ*. **2021**, *5*, 71-86.

59. Alsubih, M.; Mallick, J.; Talukdar, S.; Salam, R.; AlQadhi, S.; Fattah, M.A.; Thanh, N.V. An investigation of the short-term meteorological drought variability over Asir Region of Saudi Arabia. *Theor. Appl. Clim*. **2021**, 1-21.

60. Chong, K.; Huang, Y.; Koo, C.; Ahmed, A.N.; and El-Shafie, A. Spatiotemporal Variability Analysis of Standardized Precipitation Indexed Droughts Using Wavelet Transform. *J.Hyd*. **2021**, 127299.

61. Ullah, I.; Ma, X.; Yin, J.; Saleem, F.; Syed, S.; Omer, A.; Habtemicheal, B.A.; Liu, M.; and Arshad, M. Observed changes in seasonal drought characteristics and their possible potential drivers over Pakistan. *Int. J. Clim*. **2021**.

62. Pandey, B.K.; Khare, D.; Tiwari, H.; Mishra, P.K. Analysis and visualization of meteorological extremes in humid subtropical regions. *Nat. Haz*. **2021**, 1-27.

63. Sein, Z.M.M.; Zhi, X.; Ullah, I.; Azam, K.; Ngoma, H.; Saleem, F.; Xing, Y.; Iyakaremye, V.; Syed, S.; Hina, S. Recent variability of sub□seasonal monsoon precipitation and its potential drivers in Myanmar using in□situ observation during 1981–2020. *Int. J.Clim*. **2021**.

64. Ouyang, X.; Chen, D.; Zhou, S.; Zhang, R.; Yang, J.; Hu, G.; Dou, Y.; Liu, Q. A Slight Temperature Warming Trend Occurred over Lake Ontario from 2001 to 2018. *Lan*. **2021**, *10*, 1315.

65. Hussain, A.; Cao, J.; Ali, S.; Ullah, W.; Muhammad, S.; Hussain, I.; Rezaei, A.; Hamal, K.; Akhtar, M.; Abbas, H. Variability in runoff and responses to land and oceanic parameters in the source region of the Indus River. *Ecologic. Indic*. **2022**, *140*, 109014.

66. Yang, M.-S.; and Hussain, I. Unsupervised Multi-View K-Means Clustering Algorithm. *IEEE Access* **2023**, *11*, 13574-13593.

67. MacQueen, J. Some methods for classification and analysis of multivariate observations. In Proceedings of the Proceedings of the fifth Berkeley symposium on mathematical statistics and probability, **1967**, 281-297.

68. Shaheen, M.; ur Rehman, S.; Ghaffar, F. Correlation and congruence modulo based clustering technique and its application in energy classification. *Sustain. Comput.: Inf. Sys*. **2021**, *30*, 100561.

69. Hussain, A.; Cao, J.; Ali, S.; Ullah, W.; Muhammad, S.; Hussain, I.; Abbas, H.; Hamal, K.; Sharma, S.; Akhtar, M. Wavelet

coherence of monsoon and large□scale climate variabilities with precipitation in Pakistan. *Int.l J. Clim.* **2022**.

70. Ikuemonisan, F.E.; Ozebo, V.C.; Olatinsu, O.B. Investigation of Sentinel-1-derived land subsidence using wavelet tools and triple exponential smoothing algorithm in Lagos, Nigeria. *Environ. Ear. Sci.* **2021**, *80*, 1-17.

71. He, L.; Freudenreich, T.; Yu, W.; Pelowski, M.; Liu, T. Methodological structure for future consumer neuroscience research. *Psy. Mark.* **2021**, *38*, 1161-1181.

72. Vacha, L.; and Barunik, J. Co-movement of energy commodities revisited: Evidence from wavelet coherence analysis. *Ene. Eco*. **2012**, *34*, 241-247.

73. Grinsted, A.; Moore, J.C.; Jevrejeva, S. Application of the cross wavelet transform and wavelet coherence to geophysical time series. *Nonli.pro. geophy.* **2004**, *11*, 561-566.

74. Baudouin, J.-P.; Herzog, M.; and Petrie, C.A. Cross-validating precipitation datasets in the Indus River basin. *Hyd. Ear. Sys. Sci.* **2020**, *24*, 427-450.

75. Gottschalck, J.; Meng, J.; Rodell, M.; Houser, P. Analysis of multiple precipitation products and preliminary assessment of their impact on global land data assimilation system land surface states. *J. Hydromet.* **2005**, *6*, 573-598.

76. Safdar, F.; Khokhar, M.F.; Mahmood, F.; Khan, M.Z.A.; Arshad, M. Observed and predicted precipitation variability across Pakistan with special focus on winter and pre-monsoon precipitation. *Environ. Sci.Pollu. Res.* **2023**, *30*, 4510-4530.

77. Hussain, A.; Ali, S.; Begum, S.; Hussain, I.; Ali, H. Climate Change Perspective in Mountain Area: Impacts and Adaptations in Naltar Valley, Western Himalaya, Pakistan. *Fres. Environ. Bull.* **2019**, 6683.

78. Latif, M.; Syed, F.; Hannachi, A. Rainfall trends in the South Asian summer monsoon and its related large-scale dynamics with focus over Pakistan. *Clim. Dyn.* **2017**, *48*, 3565-3581.

79. Islam, T.; Md, A.R.; Rahman, M.; Khatun, R.; Hu, Z. Spatiotemporal trends in the frequency of daily rainfall in Bangladesh during 1975–2017. *Theor.Appl. climat.* **2020**, *141*, 869-887.

80. Yaseen, M.; Ahmad, I.; Guo, J.; Azam, M.I.; Latif, Y. Spatiotemporal Variability in the Hydrometeorological Time-Series over Upper Indus River Basin of Pakistan. *Adv. Meteor.* **2020**..

81. Iqbal, M.F.; Athar, H. Variability, trends, and teleconnections of observed precipitation over Pakistan. *Theor. appl. clim.* **2018**, *134*, 613-632.

82. Ahmed, K.; Shahid, S.; Chung, E.-S.; Ismail, T.; Wang, X.-J. Spatial distribution of secular trends in annual and seasonal precipitation over Pakistan. *Clim. Res.* **2017**, *74*, 95-107.

83. Hanif, M.; Khan, A.H.; and Adnan, S. Latitudinal precipitation characteristics and trends in Pakistan. *J.hyd.* **2013**, *492*, 266-272.

84. Ullah, W.; Wang, G.; Lou, D.; Ullah, S.; Bhatti, A.S.; Ullah, S.; Karim, A.; Hagan, D.F.T.; Ali, G. Large-scale atmospheric circulation patterns associated with extreme monsoon precipitation in Pakistan during 1981–2018. *Atmos. Res.* **2021**, *253*, 105489.

85. Niyogi, D.; Kishtawal, C.; Tripathi, S.; Govindaraju, R.S. Observational evidence that agricultural intensification and land use change may be reducing the Indian summer monsoon rainfall. *Wat. Resou. Res.* **2010**, *46*.

86. Priya, P.; Mujumdar, M.; Sabin, T.; Terray, P.; Krishnan, R. Impacts of Indo-Pacific sea surface temperature anomalies on the summer monsoon circulation and heavy precipitation over northwest India–Pakistan region during 2010. *J. Clim.* **2015**, *28*, 3714-3730.

87. Ahmad, I.; Zhang, F.; Tayyab, M.; Anjum, M.N.; Zaman, M.; Liu, J.; Farid, H.U.; Saddique, Q. Spatiotemporal analysis of precipitation variability in annual, seasonal and extreme values over upper Indus River basin. *Atmos. Res.* **2018**, *213*, 346-360.

88. Hasson, S. Future water availability from Hindukush-Karakoram-Himalaya Upper Indus Basin under conflicting climate change scenarios. *Clim.* **2016**, *4*, 40.

89. Hasson, S.; Lucarini, V.; Khan, M.R.; Petitta, M.; Bolch, T.; Gioli, G. Early 21st century snow cover state over the western river basins of the Indus River system. *Hyd. Ear. Sys. Sci.* **2014**, *18*, 4077-4100.

90. Bocchiola, D.; and Diolaiuti, G. Recent (1980–2009) evidence of climate change in the upper Karakoram, Pakistan. *Theor. appl.clim.* **2013**, *113*, 611-641.

91. Safdar, F.; Khokhar, M.F.; Mahmood, F.; Khan, M.Z.A.; Arshad, M. Observed and predicted precipitation variability across Pakistan with special focus on winter and pre-monsoon precipitation. *Environ. Sci.Pollu. Res.* **2022**, 1-21.

92. Ali, N.; Ahmad, I.; Chaudhry, A.; Raza, M. Trend analysis of precipitation data in Pakistan. *Sci. Int*. **2015**, *27*, 803-808.

93. Iqbal, Z.; Shahid, S.; Ahmed, K.; Ismail, T.; Nawaz, N. Spatial distribution of the trends in precipitation and precipitation extremes in the sub-Himalayan region of Pakistan. *Theor. appl. clim.* **2019**, *137*, 2755-2769.

94. Ahmad, W.; Fatima, A.; Awan, U.K.; Anwar, A. Analysis of long term meteorological trends in the middle and lower Indus Basin of Pakistan—A non-parametric statistical approach. *Glob. Planet. Chan*. **2014**, *122*, 282-291.

95. Nawaz, Z.; Li, X.; Chen, Y.; Guo, Y.; Wang, X.; Nawaz, N. Temporal and spatial characteristics of precipitation and temperature in Punjab, Pakistan. *Wat.* **2019**, *11*, 1916.

96. Guo, X.; Wang, L.; Tian, L. Spatio□temporal variability of vertical gradients of major meteorological observations around the Tibetan Plateau. *Int. J. Clim*. **2016**, *36*, 1901-1916.

97. Li, Z.; He, Y.; Wang, C.; Wang, X.; Xin, H.; Zhang, W.; Cao, W. Spatial and temporal trends of temperature and precipitation during 1960–2008 at the Hengduan Mountains, China. *Quat. Int.l* **2011**, *236*, 127-142.

98. Hussain, A.; Cao, J.; Hussain, I.; Begum, S.; Akhtar, M.; Wu, X.; Guan, Y.; Zhou, J. Observed Trends and Variability of Temperature and Precipitation and Their Global Teleconnections in the Upper Indus Basin, Hindukush-Karakoram-Himalaya. *Atmos*. **2021**, *12*, 973. https://doi.org/10.3390/atmos12080973

99. Hussain, M.S.; and Lee, S. The regional and the seasonal variability of extreme precipitation trends in Pakistan. *Asi.Pac. J. Atmos. Sci.* **2013**, *49*, 421-441, doi:10.1007/s13143-013-0039-5.

100. Zhou, L.; Zhu, J.; Zou, H.; Ma, S.; Li, P.; Zhang, Y.; Huo, C. Atmospheric moisture distribution and transport over the Tibetan Plateau and the impacts of the South Asian summer monsoon. *Act. Meteor. Sin*. **2013**, *27*, 819-831.

101. Zhang, R.; Jiang, D.; Zhang, Z.; Yu, E. The impact of regional uplift of the Tibetan Plateau on the Asian monsoon climate. *Palaeogeo. Palaeoclim. Palaeoeco.* **2015**, *417*, 137-150.

102. Hasson, S.; Böhner, J.; Lucarini, V. Prevailing climatic trends and runoff response from Hindukush–Karakoram–Himalaya, upper Indus Basin. *Ear. Sys. Dyn*. **2017**, *8*, 337-355.

103. Wong, K.V. *Climate change*; Momentum Press: **2015**.

104. Ullah, S.; You, Q.; Wang, G.; Ullah, W.; Sachindra, D.; Yan, Y.; Bhatti, A.S.; Abbas, A.; and Jan, M.A. Characteristics of human thermal stress in South Asia during 1981–2019. *Environ. Res. Lett.***2022**, *17*, 104018.

105. De Oliveira-Júnior, J.F.; Shah, M.; Abbas, A.; Iqbal, M.S.; Shahzad, R.; de Gois, G.; da Silva, M.V.; da Rosa Ferraz Jardim, A.M.; de Souza, A. Spatiotemporal analysis of drought and rainfall in Pakistan via Standardized Precipitation Index: homogeneous regions, trend, wavelet, and influence of El Niño-southern oscillation. *Theor. Appl. Clim.* **2022**, 1-20.

106. Attada, R.; Dasari, H.P.; Chowdary, J.S.; Yadav, R.K.; Knio, O.; Hoteit, I. Surface air temperature variability over the Arabian Peninsula and its links to circulation patterns. *Int. J.Clim.* **2019**, *39*, 445-464.

107. De Beurs, K.M.; Henebry, G.M.; Owsley, B.C.; Sokolik, I.N. Large scale climate oscillation impacts on temperature, precipitation and land surface phenology in Central Asia. *Environ. Res. Lett.* **2018**, *13*, 065018.

108. Syed, F.S.; Giorgi, F.; Pal, J.; Keay, K. Regional climate model simulation of winter climate over Central–Southwest Asia, with emphasis on NAO and ENSO effects. *Int. J.Clim.* **2010**, *30*, 220-235.